Bose-Einstein condensation: Kinetic evolution obtained from simulated trajectories

M. Holland, J. Williams, and J. Cooper
JILA and Department of Physics, University of Colorado, Boulder, Colorado 80309-0440
(Received 27 November 1996)

In this paper, we present a method for simulating the kinetic evolution of a dilute gas of atoms that are cooled below the critical temperature for Bose-Einstein condensation. Our method gives insight into the formulation of physical kinetics by illustrating directly the decomposition of the distribution function into an infinite sum of single-particle trajectories. This approach is valid for the entire range of phase-space densities, although we limit the discussion here to exclude the region where the condensate fraction is close to unity and the effect of the mean field is significant. We present explicit calculations of finite number effects on equilibrium, the dynamic build-up of the ground state, and simulations of evaporative cooling. [S1050-2947(97)06005-8]

PACS number(s): 03.75.Fi, 05.20.Dd, 32.80.Pj

I. INTRODUCTION

In recent experiments demonstrating Bose-Einstein condensation of a dilute alkali-metal vapor, the temperature of a gas was reduced by several orders of magnitude using the crucial technique of evaporative cooling [1–5]. The theoretical study of this important technique and the description of condensate formation requires a kinetic theory that treats nonequilibrium, open systems in both the classical and quantum degenerate regimes. It is also necessary to consider a system of finite size as determined by the form of the confining potential [6,7].

We present an alternative approach to describing quantum kinetics that is motivated by the quantum trajectory methods developed in quantum optics to describe the dissipative evolution of open systems [8–14]. The basic principle on which these models are built is that the evolution of the open system, described by a density operator master equation, can be obtained by accumulating an infinite number of stochastic realizations of a wave-function trajectory. A simple example of an open system is an excited atom coupled to the radiation vacuum reservoir. A trajectory in this case consists of the interruption of the continuous evolution of the atomic wave function by a quantum jump to the ground state when a spontaneous photon is emitted.

We have applied this trajectory method to a fundamentally different problem. In our case, we wish to describe the evolution of a gas of atoms that are not coupled to a reservoir at all. The jumps that occur in the single-atom trajectory that lead to the irreversible evolution of the system are caused by atomic collisions with other atoms in the gas. Thus the role of the reservoir in our problem is played by the system itself. This inherent nonlinearity is illustrated by the kinetic equation we are trying to simulate. We have previously applied this approach to treat the classical Boltzmann equation in order to describe the evaporative cooling process [15]. In this paper, we extend the theory to treat Bose-Einstein condensation.

This paper is divided into three parts. We first present the theory for kinetic evolution in Sec. II. In Sec. III, we describe our trajectory approach and outline in detail the corresponding simulation procedure. Finally, in Sec. IV, we present applications of the method for thermodynamics, condensate growth, and evaporative cooling.

II. ERGODIC QUANTUM BOLTZMANN EQUATION

In this section, we outline our mathematical description of kinetic theory and highlight the physical assumptions made in its derivation. We present the quantum Boltzmann equation (QBE), which is the starting point for our treatment. An ergodic assumption is made, which simplifies the problem by assuming that the population of a state depends only on its energy. We show how the ergodic QBE goes to the ergodic classical Boltzmann equation in the appropriate limit, a result that greatly simplifies the trajectory simulation presented in Sec. III.

A. Quantum Boltzmann equation

We consider a dilute system of atoms confined in an isotropic harmonic oscillator of frequency ω. The Hamiltonian $H=H_0+H_I$ consists of a free part H_0 and an interaction term H_I due to binary collisions

$$H_0=\sum_{\vec{n}} E_{\vec{n}} a_{\vec{n}}^{\dagger} a_{\vec{n}},$$

$$H_I=\frac{1}{2}\sum_{\vec{n},\vec{m},\vec{q},\vec{p}} C(\vec{n},\vec{m};\vec{q},\vec{p})\, a_{\vec{n}}^{\dagger} a_{\vec{m}}^{\dagger} a_{\vec{q}} a_{\vec{p}}, \tag{1}$$

where $E_{\vec{n}}=(n_x+n_y+n_z+\frac{3}{2})\hbar\omega$ is the energy eigenvalue of H_0 with quantum number $\vec{n}=(n_x,n_y,n_z)$. Here $a_{\vec{n}}$ is the annihilation operator that removes an atom from the single-particle eigenstate $\phi_{\vec{n}}$. The transition amplitude is

$$C(\vec{n},\vec{m};\vec{q},\vec{p}) = \int d^3x\, d^3x'\, \phi_{\vec{n}}^*(\vec{x})\,\phi_{\vec{m}}^*(\vec{x}')\,V(\vec{x},\vec{x}')\,\phi_{\vec{q}}(\vec{x})\,\phi_{\vec{p}}(\vec{x}'), \tag{2}$$

where $V(\vec{x},\vec{x}')$ is a two-particle potential. In the temperature range of interest, s-wave scattering predominates and collisions are characterized by a contact potential

$$V(\vec{x},\vec{x}')=\frac{4\pi\hbar^2 a}{m}\ \delta^3(\vec{x}-\vec{x}'), \tag{3}$$

where a is the scattering length. This gives the quantum-mechanical cross section for the collision $\sigma=8\pi a^2$.

The correlation time arising from the duration of a collision in Bose-Einstein condensation experiments is typically much shorter than the time scale on which the system relaxes to equilibrium. The time scale for pair correlations is given by $\tau_{\rm cor}=a/\overline{v}$, where $\overline{v}$ is the mean velocity. The relaxation time is determined by the time between elastic collisions $\tau_{\rm col}$ in the gas. For example, in the experiments described in Ref. [1], at the critical temperature $\tau_{\rm cor}\approx 1\ \mu$s, compared to $\tau_{\rm col}\approx 0.1$ s. In this regime, Wick's theorem [16–18] may be applied to give the evolution under the Born and Markov approximations of the atomic population

$$f_{\vec{n}}={\rm Tr}\{\rho a_{\vec{n}}^{\dagger}a_{\vec{n}}\}, \tag{4}$$

where ρ is the N-particle density matrix for the system. In the representation of the bare harmonic-oscillator states, off-diagonal elements $f_{\vec{n}\vec{n}'}={\rm Tr}\{\rho a_{\vec{n}}^{\dagger}a_{\vec{n}'}\}$, $\vec{n}\neq\vec{n}'$, [18] may be adiabatically eliminated when $\omega\tau_{\rm col}\gg 1$. This gives the QBE [18–22].[1]

$$\frac{\partial f_{\vec{n}}}{\partial t}=\sum_{\vec{m},\vec{q},\vec{p}} W(\vec{n},\vec{m};\vec{q},\vec{p})[f_{\vec{q}}f_{\vec{p}}(1+f_{\vec{n}})(1+f_{\vec{m}}) - f_{\vec{n}}f_{\vec{m}}(1+f_{\vec{q}})(1+f_{\vec{p}})], \tag{5}$$

where the transition rate $W(\vec{n},\vec{m};\vec{q},\vec{p})$ appearing in Eq. (5) is obtained from Fermi's golden rule

$$W(\vec{n},\vec{m};\vec{q},\vec{p})=\frac{2\pi}{\hbar}\ |C(\vec{n},\vec{m};\vec{q},\vec{p})|^2\ \frac{\delta_{E_{\vec{n}}+E_{\vec{m}},E_{\vec{q}}+E_{\vec{p}}}}{\hbar\omega} \tag{6}$$

and δ is the Kronecker delta function giving energy conservation. The total number of particles in the system N determines the normalization of $f_{\vec{n}}$ by $\Sigma_{\vec{n}}f_{\vec{n}}=N$.

B. Ergodic assumption

A practical problem for simulating the QBE is that the degeneracy of states increases rapidly with increasing energy. The degeneracy of a level for the isotropic harmonic oscillator is proportional to the square of the energy so that even for very low temperatures, the number of states whose populations must be calculated may be very large. For example, if $k_BT=10\hbar\omega$, we would have to consider approximately 10^5 states. This is a severe limitation on the computation speed.

We resolve this difficulty by assuming that the population within a degenerate subspace is uniformly distributed among the degenerate states. In other words, in the spherical basis we assume that the population $f_{\vec{n}}$ depends only on the principle quantum number n and not on the angular momentum quantum numbers l and m. This assumption is true at equilibrium since then the distribution function is purely a function of the Hamiltonian. In many cases of interest, the system remains close to equilibrium and we expect the approximation to be valid. In Ref. [23], it was shown that for a homogeneous system originally in equilibrium, if one of the three degenerate states in the first excited level is depleted and the system is allowed to evolve back to equilibrium, the population gets redistributed equally among the three degenerate states in a time on the order of the mean collision time in the gas.

This ergodic assumption is defined as

$$f_{\vec{n}}=\sum_{\epsilon_n}\ \delta_{\epsilon_n,E_{\vec{n}}}\ f_{\epsilon_n}. \tag{7}$$

Each state $\phi_{\vec{n}}$ in the degenerate subspace has the same population f_{ϵ_n}. Therefore, a sum over all of the degenerate states is just

$$g_{\epsilon_n}\ f_{\epsilon_n}=\sum_{\vec{n}}\ \delta_{\epsilon_n,E_{\vec{n}}}\ f_{\vec{n}}, \tag{8}$$

where g_{ϵ_n} is the degeneracy of energy level ϵ_n, which is given by

$$g_{\epsilon_n}=\frac{1}{2}\ (n+1)(n+2). \tag{9}$$

With the ergodic assumption, Eq. (5) can be reduced to

$$g_{\epsilon_n}\frac{\partial f_{\epsilon_n}}{\partial t}=\sum_{\epsilon_m,\epsilon_q,\epsilon_p} W(\epsilon_n,\epsilon_m;\epsilon_q,\epsilon_p)[f_{\epsilon_q}f_{\epsilon_p}(1+f_{\epsilon_n}) \times(1+f_{\epsilon_m})-f_{\epsilon_n}f_{\epsilon_m}(1+f_{\epsilon_q})(1+f_{\epsilon_p})]. \tag{10}$$

The collision kernel $W(\epsilon_n,\epsilon_m;\epsilon_q,\epsilon_p)$ is now a sum over all of the rates corresponding to the possible degenerate states that could participate in the collision,

$$W(\epsilon_n,\epsilon_m;\epsilon_q,\epsilon_p) =\frac{2\pi}{\hbar}\ \frac{\delta_{\epsilon_n+\epsilon_m,\epsilon_q+\epsilon_p}}{\hbar\omega}\ \sum_{\vec{n},\vec{m},\vec{q},\vec{p}}\left(|C(\vec{n},\vec{m};\vec{q},\vec{p})|^2\prod_j\ \delta_{\epsilon_j,E_{\vec{j}}}\right), \tag{11}$$

where $j\in\{n,m,q,p\}$ in the product. The normalization of the distribution becomes $\Sigma_{\epsilon_n}g_{\epsilon_n}f_{\epsilon_n}=N$.

We have made a great simplification by reducing the QBE to Eq. (10). Considering our previous example of $k_BT=10\hbar\omega$, the number of levels occupied is approximately 100, which is much less than the corresponding number of states 10^5.

[1]Note that the use of Wick's theorem makes it possible to use single-particle trajectories to simulate the mean number of atoms, whose time evolution is given by Eq. (5). This is in contrast with the kinetic equation that is simulated in Ref. [23] by Jaksch *et al.* Although similar in form to Eq. (5), their equation gives the time evolution of a single realization out of the microcanonical ensemble for an N-body system.

C. Classical limit

Although the ergodic assumption presented in Sec. II B greatly simplifies the problem of simulating the QBE, it is desirable to reduce the problem further in order to describe the evaporative cooling technique used to reach the critical density for Bose-Einstein condensation. During the evaporation process, the temperature of the gas is reduced by several orders of magnitude. Even with the ergodic assumption, a very large number of energy levels must be considered to describe the system in this entire range. The process can be described by the classical Boltzmann equation for most of this range, down to some point close to the critical temperature when quantum statistics becomes important. In this critical region, the QBE must be used.

The problem may be simplified if a smooth transition connecting these two regions can be found, which would allow energy levels above some cutoff to be treated classically. Taking the classical limit of Eq. (10) corresponds to taking $\epsilon_n \to \infty$ and assuming that $T > T_c$ so that the $1+f_{\epsilon_n}$ Bose-enhancement factors go to unity.

Equation (10) can be written in dimensionless form

$$g_{e_n}\frac{\partial f_{e_n}}{\partial \tau} = \sum_{e_m,e_q,e_p} \delta_{e_n+e_m,e_q+e_p} g(e_n,e_m;e_q,e_p) \times [f_{e_q} f_{e_p}(1+f_{e_n})(1+f_{e_m}) - f_{e_n} f_{e_m}(1+f_{e_q})(1+f_{e_p})], \tag{12}$$

where time and energy are in the natural units of the problem, $\tau = (m\sigma\omega^2/\pi^2\hbar)\,t$ and $e_n = \epsilon_n/\hbar\omega$. The collision kernel given in Eq. (11) is now dimensionless and given by

$$g(e_n,e_m;e_q,e_p) = \frac{4}{\pi^2}\sum_{\vec{n},\vec{m},\vec{q},\vec{p}} \left(\left| \prod_i N_{n_i} N_{m_i} N_{q_i} N_{p_i} I_{n_i m_i q_i p_i} \right|^2 \prod_j \delta_{e_j,E_{\vec{j}}} \right), \tag{13}$$

where $i \in \{x,y,z\}$ in the first product and $N_{n_i} = (2^{n_i} n_i!)^{-1/2}$ is the normalization factor for component i of the state $\phi_{\vec{n}}$. The overlap integral of the four Hermite polynomials $H_{n_i}(u_i)$ is

$$I_{n_i m_i q_i p_i} = \int du_i H_{n_i} H_{m_i} H_{q_i} H_{p_i} e^{-2u_i^2}. \tag{14}$$

In taking the limit $e_n \to \infty$, f_{e_n} is replaced by a continuous function of energy $f(e_n)$, each sum over e_n is replaced by an integral, and the Kronecker δ is replaced by a Dirac δ. For temperatures well above T_c, the Bose-enhancement factors $1+f_{e_n}$ can be set equal to unity. The collision kernel $g(e_n,e_m;e_q,e_p)$ has a rather simple limiting form, which may be found by computing numerically the quantity on the right-hand side of Eq. (13). We use the following expression for the overlap integral [24]:

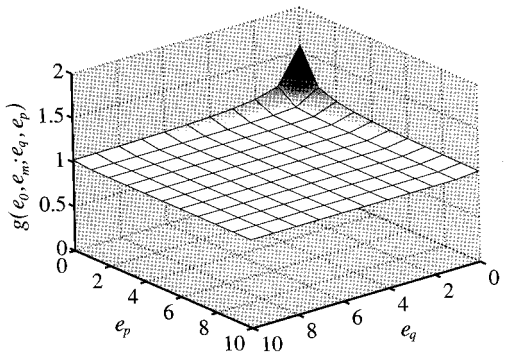

FIG. 1. Plot of $g(e_{\min},e_m;e_q,e_p)$ vs (e_q,e_p) for the minimum energy being in the ground state $e_{\min}=e_0$, where e_m is determined by energy conservation. It is a very flat function, differing from its asymptotic form $g_{e_0}=1$, only when Δ_e is very small.

$$I_{nmqp} = \frac{m!n!}{\pi}\sum_{t=0}^{\min(m,n)} \frac{2^t}{t!(m-t)!(n-t)!}\,2^{k-1/2} \times \Gamma(k-p+\tfrac{1}{2})\Gamma(k-m-n+2t+\tfrac{1}{2})\Gamma(k-q+\tfrac{1}{2}), \tag{15}$$

where $2k = \sigma_n - 2t$ and $\sigma_n = n+m+p+q$ must be even. The integral is zero if σ_n is odd.

We calculated the kernel $g(e_n,e_m;e_q,e_p)$ numerically for $e_0 \leq e_j \leq e_{20}$, where $e_j \in \{e_n,e_m,e_q,e_p\}$, and obtained a remarkable result. This collision kernel converges very quickly to the degeneracy g_{e_n}, given by Eq. (9), as the differences $\Delta_e \equiv e_j - e_{\min}$ between the minimum energy and the other three energies increase

$$g(e_{\min},e_m;e_q,e_p) \xrightarrow[\Delta_e \to \infty]{} g_{e_{\min}}, \tag{16}$$

where $e_{\min} = \min\{e_n,e_m,e_q,e_p\}$ is the minimum energy. Figure 1 shows a plot of $g(e_{\min},e_m;e_q,e_p)$ vs (e_p,e_q) for $e_{\min}=e_0$, with e_m determined by energy conservation. It is a very flat function differing from its asymptotic form only when Δ_e is very small. From our calculations, we found that the convergence in Eq. (16) becomes faster as $e_{\min}$ increases. Furthermore, as e_j increases, the degeneracy factor g_{e_j} converges to the density of states $\rho(e_j) \equiv (1/2)e_j^2$

$$g_{e_j} \underset{e_j \to \infty}{\to} \rho(e_j). \tag{17}$$

In our simulation procedure described below, we use the limiting form Eq. (16) for $g(e_n,e_m;e_q,e_p)$ when any one of the energies is greater than the tenth level e_{10} and use the limiting form Eq. (17) when all of the energies are greater than a cutoff energy e_c chosen such that $(1+f_{e_c}) \approx 1$.

The comparison with the ergodic classical Boltzmann equation can now be made. The classical limit of Eq. (12) is

$$\rho(e_n)\frac{\partial f(e_n)}{\partial \tau} = \int de_m de_q de_p\, \delta(e_n+e_m-e_q-e_p)\rho(e_{\min}) \times [f(e_q)f(e_p) - f(e_n)f(e_m)], \tag{18}$$

where the same natural units given below Eq. (12) are used here. This agrees with the classical Boltzmann equation given by Eq. (14) in Ref. [6].

III. TRAJECTORY SIMULATION

In this section, we explain our approach to simulating the QBE using simulated single-particle trajectories. We first show that the time evolution of f_{e_n} given by Eq. (12) can be described by a sum over all possible single-particle trajectories. We then outline the specific simulation procedure.

A. Trajectory decomposition of the QBE

We can now incorporate quantum statistics into the trajectory method using the results of Sec. II. We cannot expect the simulation to be valid far below the critical temperature when a large proportion of atoms are in the ground state since we neglect the effect of the mean field on the system and work in the representation of the bare harmonic-oscillator basis. However, in the regime where $\omega\tau_{\rm col}\gg 1$ holds, the buildup of the condensate can still be investigated. This simulation method is now ideal for describing the evaporative cooling of atoms all the way down to temperatures below T_c.

The trajectory decomposition of the ergodic QBE closely resembles that given in Ref. [15] for the classical case. Still working in the natural units of time and energy given below Eq. (12), we begin by defining a trajectory function $f(e_n,t|t_\eta,e_\eta,\ldots,t_1,e_1)$, which describes a specific collision history with energy e_n at time t: The trajectory is labeled by its history of η collisions occurring at times $t_1,\ldots,t_\eta$, with $t>t_\eta>\cdots>t_1$, and with the energy before each collision given by $e_1,\ldots,e_\eta$.

Our task is to correctly describe the time evolution of this trajectory function so that upon accumulating all possible realizations of trajectories, $f_{e_n}(t)$ is attained with the correct time evolution governed by Eq. (12). To obtain $f_{e_n}(t)$ from the accumulated trajectories, we form a distribution of the energies collected from M trajectories at the particular time t. Then in the limit $M\to\infty$, the distribution should converge upon $f_{e_n}(t)$. Realistically, the number of trajectories we accumulate is in the range 10^4-10^5. Of course, the trajectories must be weighted so that the final distribution obtained from the accumulated trajectories is normalized to N.

This sum over trajectories can be written explicitly as

$$g_{e_n}f_{e_n}(t)=\sum_{\eta=0}^{\infty}\sum_{e_\eta,\ldots,e_1}\int_{t_0}^{t}dt_\eta\int_{t_0}^{t_\eta}dt_{\eta-1}\cdots \times\int_{t_0}^{t_2}dt_1 f(e_n,t|t_\eta,e_\eta,\ldots,t_1,e_1), \quad (19)$$

where we sum over the number η of possible collisions, sum over all possible energies occurring before each collision, and integrate over the possible times at which each collision can occur. Each trajectory has a weight given by N/M, where M goes to infinity in Eq. (19).

The time evolution of $f_{e_n}(t)$ in terms of the trajectory decomposition is found by differentiating Eq. (19)

$$g_{e_n}\frac{\partial f_{e_n}(t)}{\partial t}=\sum_{\eta=0}^{\infty}\sum_{e_\eta,\ldots,e_1}\left\{\int_{t_0}^{t}dt_\eta\cdots \times\int_{t_0}^{t_2}dt_1\frac{\partial f(e_n,t|t_\eta,e_\eta,\ldots)}{\partial t} +\int_{t_0}^{t}dt_{\eta-1}\cdots\int_{t_0}^{t_2}dt_1 f(e_n,t|t,e_\eta,\ldots)\right\}. \quad (20)$$

We must find the correct time evolution of the trajectory function $f(e_n,t|t_\eta,e_\eta,\ldots,t_1,e_1)$ so that the time evolution given by this decomposition is equivalent to the QBE. The first term on the RHS of Eq. (20) gives the time evolution of the trajectory between collisions, while the second term is related to the instantaneous change in the trajectory's energy when a collision occurs.

Between collisions, the trajectory's norm will decay due to the probability for a collision to occur with an atom from the rest of the gas

$$\frac{\partial f(e_n,t|t_\eta,e_\eta,\ldots)}{\partial t}=-\gamma(e_n,t)f(e_n,t|t_\eta,e_\eta,\ldots). \quad (21)$$

The rate of decay $\gamma(e_n,t)$ is equal to the collision rate. A particle in the system with energy e_n has a rate of colliding with any other particle in the system given by

$$\gamma(e_n,t)=\sum_{e_m,e_q,e_p}\delta_{e_n+e_m,e_q+e_p}\frac{g(e_n,e_m;e_p,e_q)}{g_{e_n}} \times f_{e_m}(t)[1+f_{e_q}(t)][1+f_{e_p}(t)]. \quad (22)$$

Because of Bose statistics, some of the collisions will be enhanced by the factors $1+f_{e_q}(t)$ if the populations in those output channels are large. This dependence on the population in summing over the output channels is absent in the trajectory method presented for the classical Boltzmann equation in Ref. [15]. In that case, the integrals over the output channels can be done analytically, which makes the problem scale linearly with the number of energy bins used to store $f(e)$. We cannot make that simplification here.

The function $f(e_n,t|t,e_\eta,\ldots)$ indicates that a collision has occurred at time t, changing the energy from e_η to e_n. We interpret the function $f(e_n,t|t,e_\eta,\ldots)$ as the rate that a particle with energy e_η will collide with any atom in the system and attain the energy e_n afterwards. Thus $f(e_n,t|t,e_\eta,\ldots)$ can be obtained by omitting the sum over the output channel e_n in Eq. (22) and weighting the rate by the norm of the trajectory before the collision

$$f(e_n,t|t,e_\eta,\ldots)=\sum_{e_m,e_p}\delta_{e_\eta+e_p,e_n+e_m}\frac{g(e_\eta,e_p;e_n,e_m)}{g_{e_\eta}} \times f_{e_p}(t)[1+f_{e_n}(t)] \times[1+f_{e_m}(t)]f(e_\eta,t|t_{\eta-1},e_{\eta-1},\ldots). \quad (23)$$

With the above description of the time evolution of a trajectory, one can easily verify that the decomposition in Eq. (20) is equivalent to Eq. (12) by substituting Eq. (21)–(23) into Eq. (20) and using Eq. (19) to reduce the expression.

One crucial point, however, has not been addressed in our proof. Because the rates given in Eqs. (22) and Eq. (23) depend on $f_{e_n}(t)$, which is the quantity being calculated, the problem is nonlinear and must be solved self-consistently. A self-consistent solution can be found if we make the incremental time of evolution dt much smaller than the mean collision time $\tau_{\rm col}$, so that $f_{e_n}(t)$ does not change appreciably during the coarse-grained time steps.

B. Simulation procedure

We now describe the procedure for simulating the QBE using the trajectory method. One begins by creating the initial distribution $f_{e_n}(t_0)$, the time evolution of which is desired over a chosen time interval. This distribution is evolved incrementally, by adding up M trajectories over a time interval dt that must be chosen smaller than the average single-particle collision time $\tau_{\rm col}$. Then, the simulated distribution at the end of the time t_0+dt is used as the starting distribution for the next time step, and so on, until the desired time is reached. In more detail, this procedure is as follows:

(i) Create an empty distribution function $f_{e_n}(t_0+dt)$ with zero population throughout the levels.

(ii) Choose an initial energy e_1 for the trajectory from the initial distribution $g_{e_n}f_{e_n}(t_0)$.

(iii) Calculate the initial collision rate $\gamma(e_1,t_0)$ using $f_{e_n}(t_0)$ for the distribution:

$$\gamma(e_1,t_0)=\sum_{e_m,e_q,e_p}\delta_{e_1+e_m,e_q+e_p}\,\frac{g(e_1,e_m;e_p,e_q)}{g_{e_1}}\times f_{e_m}(t_0)[1+f_{e_q}(t_0)][1+f_{e_p}(t_0)]. \tag{24}$$

(iv) Simulate a realization of a uniform random variable $R_1\in[0,1]$ and find the time the particle will next collide given by $t_c=t_0-\ln(R_1)/\gamma(e_1,t_0)$

(v) If $t_c>t_0+dt$, record the atom in $f_{e_n}(t_0+dt)$ by incrementing the level corresponding to its energy by the amount N/M.

(vi) If $t<t_0+dt$, a collision occurs. Simulate a second random variable $R_2\in[0,1]$. The energy after the collision is found from the solution of $e_{\rm sim}$ in

$$\sum_{e_n}^{e_{\rm sim}}\sum_{e_m,e_p}\delta_{e_1+e_p,e_n+e_m}\,\frac{g(e_1,e_p;e_n,e_m)}{g_{e_1}}\,f_{e_p}(t_0)\times[1+f_{e_n}(t_0)][1+f_{e_m}(t_0)]=R_2\gamma(e_1,t_0). \tag{25}$$

(vii) Continue steps (iii)–(vi) until the end of the interval t_0+dt is reached. Because dt must be much smaller than $\tau_{\rm col}$, multiple collisions should be rare.

(viii) Calculate the next trajectory by choosing another initial energy in step (ii) and carrying out steps (iii)–(vii). Continue the process for M trajectories.

(ix) When all of the trajectories have been accumulated, a good approximation to $f_{e_n}(t_0+dt)$ has been determined.

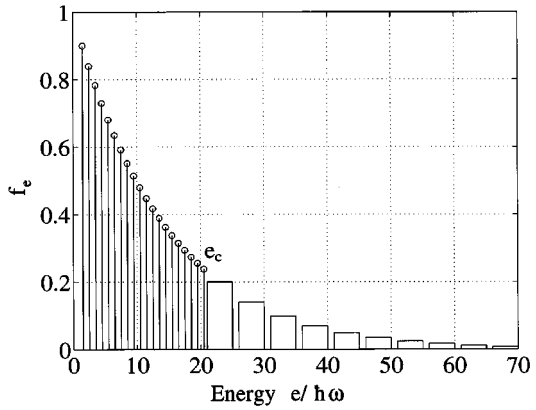

FIG. 2. Illustration of the distribution of populations f_e over the discrete and continuous regions. Above the cutoff e_c, we drop the $1+f_{e_n}$ factors and the levels are put in bins as though they formed a continuous spectrum.

One can then move on to the next time step and repeat steps (i)–(viii) by using $f_{e_n}(t_0+dt)$ as the initial distribution. This coarse-grained time evolution can be continued until $f_{e_n}(t)$ has been obtained for the desired time duration.

This trajectory simulation scales quadratically with the number of levels whose populations must be stored, which is an improvement over the cubic scaling of a direct numerical integration of Eq. (12). However, as already pointed out, the trajectory simulation of the classical Boltzmann equation scales linearly with the number of bins used to store $f(e)$. It is now very clear that making the ergodic assumption and using the classical, limiting form of the ergodic, QBE will increase the speed of the simulation enormously by decreasing the number of discrete energy levels whose populations must be simulated. By treating most of the levels above some cutoff e_c classically according to Eq. (18), the linear scaling of the method described in Ref. [15] can almost be restored. The cutoff is chosen so that $f_{e_c}\ll 1$. Because e_c increases with the number of atoms in the gas, it becomes increasingly difficult to simulate the QBE as N increases.

In order to speed up the simulation by using the smooth transition to the ergodic, classical Boltzmann equation described in Sec. II C, we use a distribution that has discrete levels below a cutoff energy e_c and a continuous spectrum of energies above this point, as shown in Fig. 2. Below e_c, we retain the $1+f_{e_n}$ factors. We also use $g(e_n,e_m;e_q,e_p)$ if all four energies are less than or equal to e_{10} and use its limiting form $g_{e_{\rm min}}$ if any of the four energies is greater than e_{10}. Above e_c, we drop the $1+f_{e_n}$ factors and use the density of states $\rho(e)$ as the limiting form of the degeneracy factor. When all four energies are above e_c, the simplifications made on the integrals in the collision rate, shown in Ref. [15], can be used.

IV. SIMULATION RESULTS

In this section, we carry out the simulation procedure described in Sec. III to investigate physical properties of a condensing gas of atoms trapped in an isotropic, harmonic potential. We show results demonstrating the equilibrium properties of a finite system, the build-up of the ground state

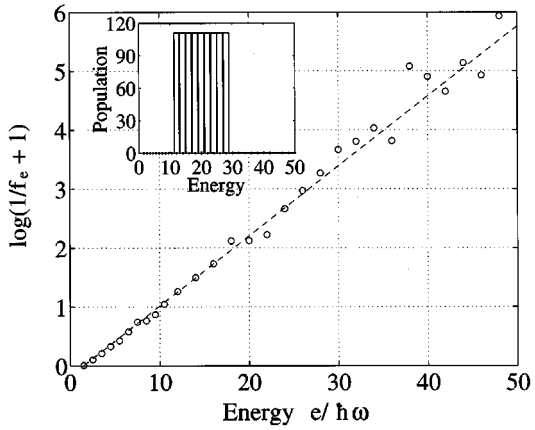

FIG. 3. System evolves to equilibrium from the distribution shown in the inset, where a single trajectory has on average 100 collisions. The final, stationary distribution (circles) agrees with the Bose-Einstein equilibrium distribution (dashes) (the natural log was used).

population starting from zero, and evaporative cooling of atoms in the trap.

A simple test of the trajectory simulation is to start the distribution $f_{e_n}(t_0)$ in a non-equilibrium state and allow it to evolve to equilibrium. In the inset of Fig. 3, the initial nonequilibrium distribution is shown for $N=10^3$ and a mean energy of $20.5\hbar\omega$. It is allowed to evolve to the stationary state shown in Fig. 3, where each trajectory had, on average, 100 collisions. The simulation data are compared with the Bose-Einstein equilibrium distribution

$$f_{e_n}=\frac{1}{e^{\beta(e_n-\mu)}-1}, \tag{26}$$

where $\beta=1/k_BT$ and μ is the chemical potential. Both β and μ are chosen in the plot so that $g_{e_n}f_{e_n}$ is normalized to N and the mean energy matches that of the simulated distribution. As Fig. 3 shows, the trajectory simulation evolves $f_{e_n}(t_0)$ to

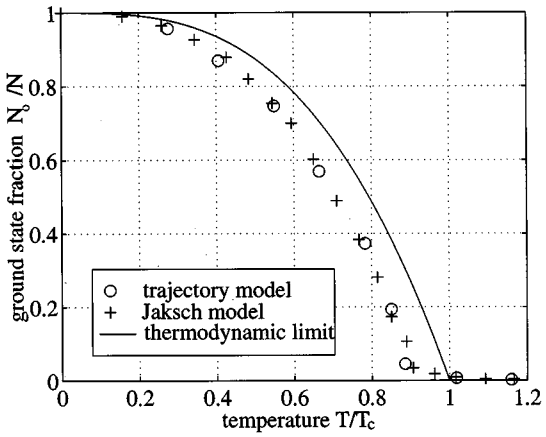

FIG. 4. Each point is obtained by allowing a system of 500 atoms with a known mean energy to evolve to equilibrium. Once equilibrium is obtained, the fraction in the ground state is recorded. The plot shows our data, data from Ref. [23], and the thermodynamic limit.

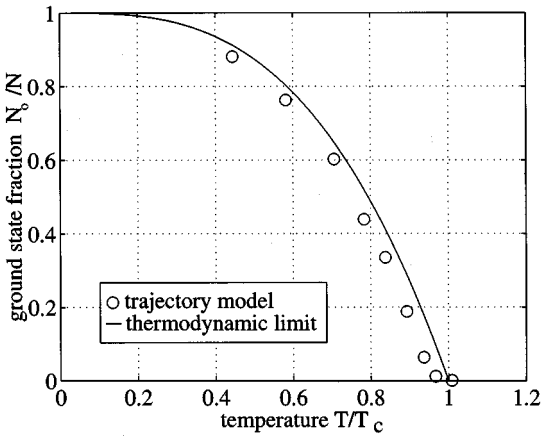

FIG. 5. Same procedure as in Fig. 4, but with 2×10^4 atoms.

the correct equilibrium distribution for a finite number of atoms without a mean field interaction.

A. Finite-number effects on equilibrium

Finite-number effects can be studied by allowing the distribution $f_{e_n}(t)$ to evolve to equilibrium. In Fig. 4, the ground-state fraction is plotted vs the temperature for the case of $N=500$. The graph shows three different sets of data: the trajectory simulation, results from Ref. [23], and the thermodynamic limit. The trajectory data agree with the results of Ref. [23], where a different approach to simulating the QBE is used. The line for a finite number of atoms has the same qualitative shape as in the thermodynamic limit, but it is shifted toward lower temperatures [23,25,26]. In Fig. 5, the same plot is shown for the case of 2×10^4 atoms. As expected, the line is shifted less from the thermodynamic limit.

The effect of finite size on the mean energy of the system can also be studied. In Fig. 6, the mean energy is plotted vs. temperature for the case of $N=500$. Again, the trajectory simulation agrees with the results of Ref. [23]. The same plot is shown in Fig. 7 for the case of 2×10^4 atoms. The mean energy for a finite number of atoms is larger than that in the

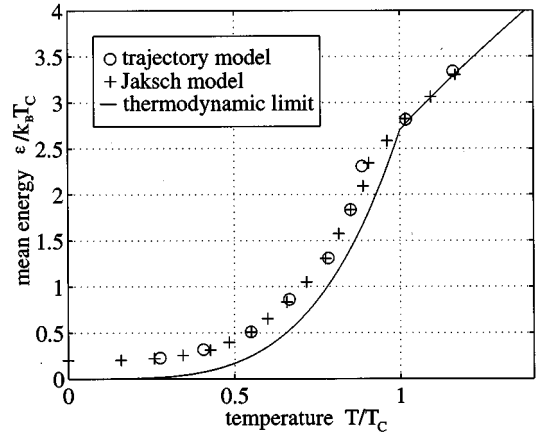

FIG. 6. Each point is obtained by allowing a system of 500 atoms with a known mean energy to evolve to equilibrium. The plot shows our data, data from Ref. [23], and the thermodynamic limit.

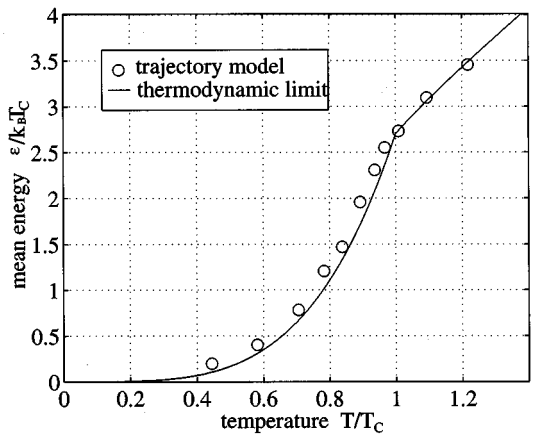

FIG. 7. Same procedure as in Fig. 6, but with 2×10^4 atoms.

thermodynamic limit below T_c. In the thermodynamic limit, the number and volume are taken to infinity, with the local density held fixed. For the case of atoms in a trap, taking the volume to infinity is achieved by allowing ω to go to zero. For a finite system, the effect of the potential remains, thus giving the system a higher mean energy than it would in the limit of $\omega\rightarrow0$.

B. Dynamic buildup of the condensate

The buildup of the condensate can be investigated by starting in a nonequilibrium distribution f_{e_n} with no atoms in the ground state initially and allowing the distribution to evolve to equilibrium. One can monitor the occupation of the ground state over time. As Fig. 8 shows, the time dependence of the population in the ground state is given by $N_0(t)=N_0(\infty)(1-e^{-t/\tau_0})$, where the time constant τ_0 is determined by fitting the data. This result also agrees with that given in Ref. [23]. The initial distribution, shown in the inset in Fig. 8, had 100 atoms with 10% in the ground state after it had reached equilibrium.

It was found that τ_0 depends slightly on the initial distribution: With the mean energy and total number fixed, the further the atoms are from e_0, the longer it will take to reach the ground state. This is also why the time constant τ_0 decreases as $N_0(\infty)$ increases while keeping N fixed, since the mean energy decreases, requiring atoms to reside in levels closer to e_0. As N gets large, more energy levels will be occupied and one might expect there to be a delay time for the atoms to begin filling the ground state [23]. Finally, it was found that $\tau_0/\tau_{\rm col}$ increases with increasing N, while keeping $N_0(\infty)/N$ fixed [27]. For the case of 100 atoms shown in Fig. 8, $\tau_0/\tau_{\rm col}\approx25$, compared to a separate case for 50 atoms, where $\tau_0/\tau_{\rm col}\approx10$.

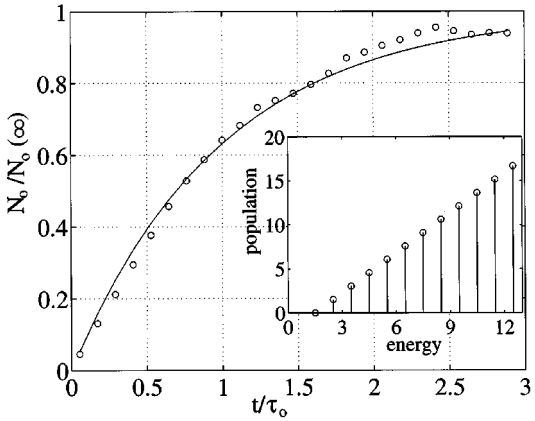

FIG. 8. Population in the ground state increases as the system of 100 atoms evolves to equilibrium, starting in the initial distribution shown in the inset (where energy is given in units of $\hbar\omega$). The ground-state fraction increases according to $N_0(t)=N_0(\infty)(1-e^{-t/\tau_0})$.

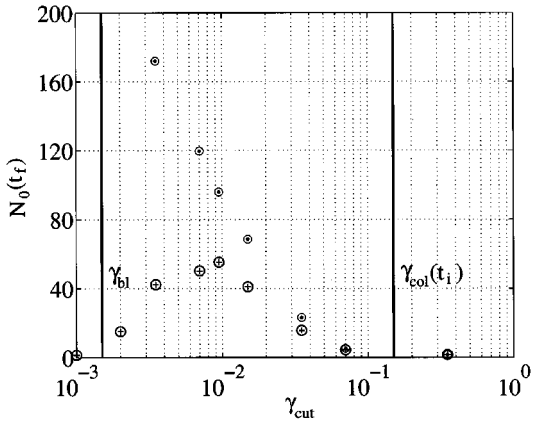

FIG. 9. Plot of the final number in the ground state $N_0(t_f)$ as a function of the cut rate $\gamma_{\rm cut}$, with (circled cross) and without (circled dot) background loss. The cut rate must be slower than the initial single-particle collision rate $\gamma_{\rm col}(t_i)$ and faster than the background loss rate $\gamma_{\rm bl}$ for the evaporation to be successful.

C. Evaporative cooling simulation

A practical use of our simulation method is to study the evaporative cooling of a gas of atoms in an isotropic harmonic trap. Evaporative cooling may be described by allowing trajectories with an energy above a time-dependent energy threshold $e_{\rm cut}(t)$ to be lost from the trap. We can also allow there to be a finite probability for trajectories to be lost due to collisions with background atoms, which occur at a rate $\gamma_{\rm bl}$.

In Fig. 9, we show data points collected from simulations of a particular evaporative cooling scenario. We began with $N=10^4$ atoms in thermal equilibrium at a temperature $T=15T_c$. We then allowed the system to evolve while lowering the energy threshold $e_{\rm cut}(t)$ exponentially in time at a rate $\gamma_{\rm cut}$, with no background losses. As the temperature approached T_c, when there was one atom in the ground state with 500 atoms left in the trap, we stopped the simulation. We then proceeded cutting exponentially to $e_{\rm cut}(t_f)=e_2$, the second energy level, at varying rates $\gamma_{\rm cut}$, as well as with and without background loss. Figure 9 shows a semilogarithmic plot of the final number in the ground state $N_0(t_f)$ vs $\gamma_{\rm cut}$.

The result is intuitive. With no background loss, $N_0(t_f)$ decreases as the cut rate increases. If we cut faster than the collision rate $\gamma_{\rm col}$, then the evaporation completely fails because the gas does not have time to equilibrate as the threshold is lowered. When background loss is included, one can see that the lower limit on $\gamma_{\rm cut}$ is determined by the back-

ground loss rate γ_{bl}. If we cut slower than the background loss rate, all of the atoms are lost from the trap before the evaporation process is finished. Thus there is an optimum cut rate γ_{cut} bracketed by these two physical properties.

V. CONCLUSION

We have presented an alternative approach to treating quantum kinetics that is based on a decomposition of the ergodic QBE into single-particle trajectories. We presented the underlying physical theory, explained our trajectory approach to simulating quantum kinetics, and displayed results of our method applied to some contemporary problems concerning Bose-Einstein condensation. As a test of the validity of our method, it agrees well with independent studies on the processes studied in Sec. IV [23]. Our approach gives an efficient simulation of quantum kinetics and is valid for the entire range of phase-space densities, excluding at this stage the region close to $T=0$ when the mean field effect on the system must be considered.

The trajectory approach of quantum kinetics described in this paper is applicable to many problems of interest. One such problem is that of finding the optimum way to lower $e_{cut}(t)$ during the evaporative cooling process with a condensate present, while taking into account all of the various loss mechanisms, such as heating due to two-body and three-body inelastic collisions. Another interesting problem is that of including the mean field effect on the system during the kinetic evolution close to $T=0$. To address this problem using the QBE, we will have to work in the representation of the mean-field states, which requires finding the mean-field eigenstates self-consistently after each time step in the simulation. Finally, it may also be interesting to use the trajectory approach to treat Fermi-Dirac statistics and describe the time evolution of a gas of fermions.

ACKNOWLEDGMENTS

We would like to thank D. Jaksch, P. Zoller, and C. Gardiner for insightful discussions on quantum kinetic theory. This work was supported by the National Science Foundation.

[1] M. H. Anderson *et al.*, Science **269**, 198 (1995).
[2] C. Bradley, C. A. Sackett, J. J. Tollett, and R. G. Hulet, Phys. Rev. Lett. **75**, 1687 (1995).
[3] K. B. Davis *et al.*, Phys. Rev. Lett. **75**, 3969 (1995).
[4] M.-O. Mewes *et al.*, Phys. Rev. Lett. **77**, 416 (1996).
[5] C. J. Myatt *et al.*, Phys. Rev. Lett. **78**, 586 (1997).
[6] O. Luiten, M. Reynolds, and J. Walraven, Phys. Rev. A **53**, 381 (1996).
[7] W. Ketterle and N. J. V. Druten, in *Advances in Atomic, Molecular, and Optical Physics* (Academic, New York, 1996), Vol. 37, p. 181.
[8] R. Dum, P. Zoller, and H. Ritsch, Phys. Rev. A **45**, 4879 (1992).
[9] C. W. Gardiner, A. S. Parkins, and P. Zoller, Phys. Rev. A **46**, 4363 (1992).
[10] R. Dum, A. S. Parkins, P. Zoller, and C. W. Gardiner, Phys. Rev. A **46**, 4382 (1992).
[11] J. Dalibard, Y. Castin, and K. Mølmer, Phys. Rev. Lett. **68**, 580 (1992).
[12] K. Mølmer, Aarhus University, Institute of Physics and Astronomy Report No. 94/08, 1994 (unpublished).
[13] H. J. Carmichael, *An Open Systems Approach to Quantum Optics* (Springer-Verlag, Berlin, 1993).
[14] N. Gisin and I. C. Percival, Phys. Lett. A **167**, 315 (1992).
[15] M. Holland, J. Williams, K. Coakley, and J. Cooper, Quantum Semiclass. Opt. **8**, 571 (1996).
[16] W. H. Louisell, *Quantum Statistical Properties of Radiation* (Wiley, New York, 1973).
[17] J. P. Blaizot and G. Ripka, *Quantum Theory of Finite Systems* (MIT Press, Cambridge, WA, 1986).
[18] A. I. Akhiezer and S. V. Peletminskii, *Methods of Statistical Physics* (Pergamon, New York, 1981).
[19] C. W. Gardiner and P. Zoller (unpublished).
[20] C. W. Gardiner and P. Zoller (unpublished).
[21] D. W. Snoke and J. P. Wolfe, Phys. Rev. B **39**, 4030 (1989).
[22] Y. M. Kagan, B. V. Svistunov, and G. V. Shlyapnikov, Zh. Eksp. Teor. Fiz. **101**, 528 (1992) [JETP **75**, 387 (1992)].
[23] D. Jaksch, C. W. Gardiner, and P. Zoller (unpublished).
[24] I. W. Busbridge, London Math. Soc. J. **23**, 135 (1948).
[25] S. Giorgini, L. P. Pitaevskii, and S. Stringari (unpublished).
[26] W. Ketterle and N. J. van Druten, Phys. Rev. A **54**, 656 (1996).
[27] D. W. Snoke and J. P. Wolfe, Phys. Rev. B **39**, 4030 (1989).